# Experimental and Theoretical X-ray Wavelengths of Astrophysical Ions

M. F. Gu[1], P. Beiersdorfer[1], G. V. Brown[1], H. Chen[1], D. B. Thorn[1], and S. M. Kahn[2]

[1]Lawrence Livermore National Laboratory, CA 94550

[2]Department of Physics, Stanford University, CA 94305

## Outline

- LLNL EBIT measurements of X-ray wavelengths, old and new.
- Many-body perturbation theory for open-shell ions.
- MBPT calculations for Fe and Ni L-shell ions.
- MBPT calculations for Fe UTA transitions.
- Summary and Future work.

# The LLNL Electron Beam Ion Trap

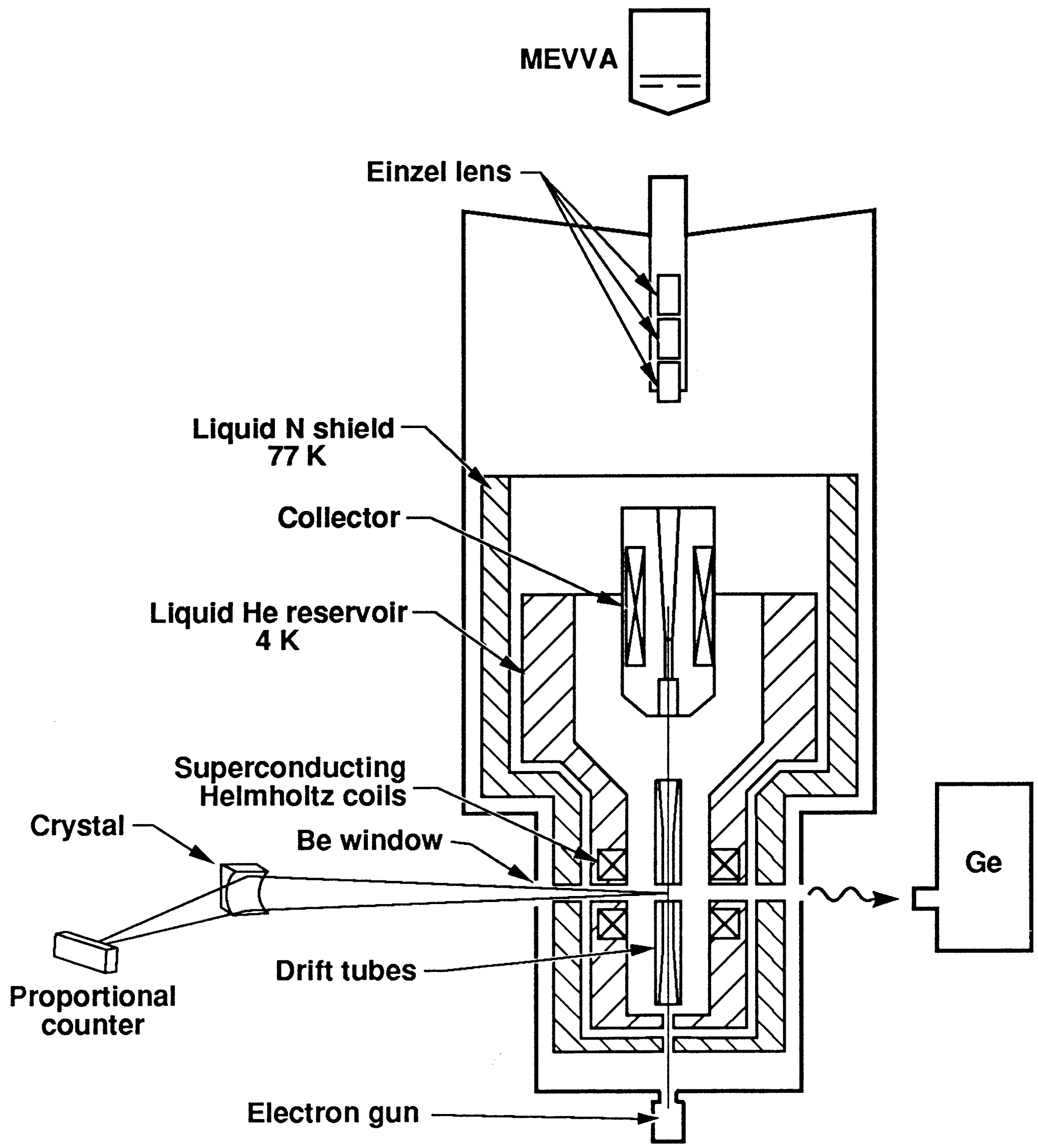

## LLNL EBIT Measurements of Fe XVII Wavelengths

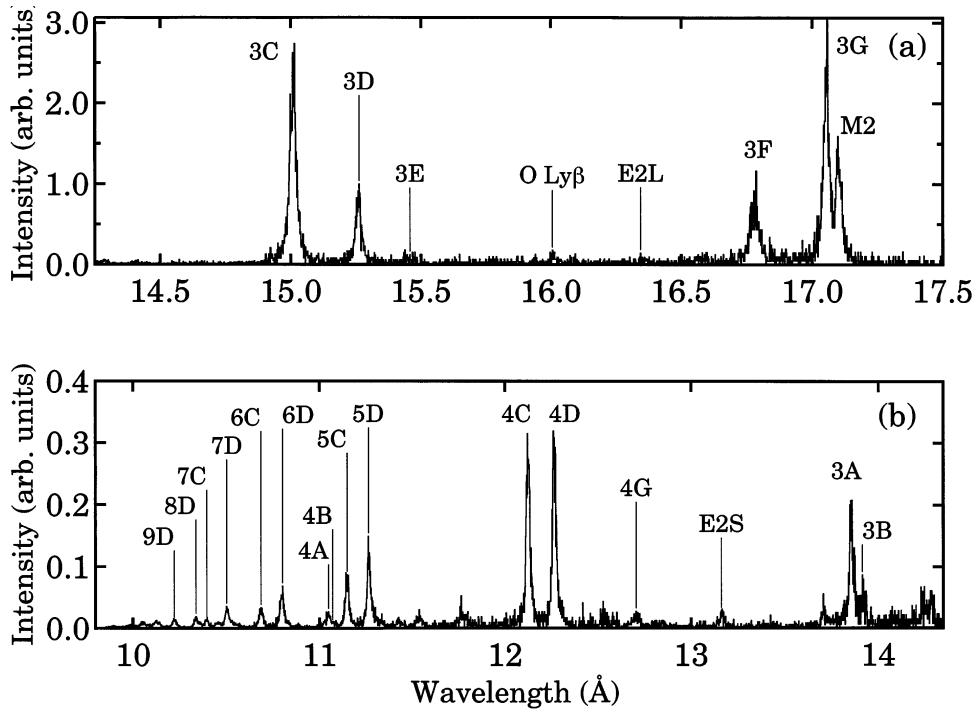


Brown et al., 1998

## Fe XVIII–XXIV above 10.6 Å, Brown et al., 2002

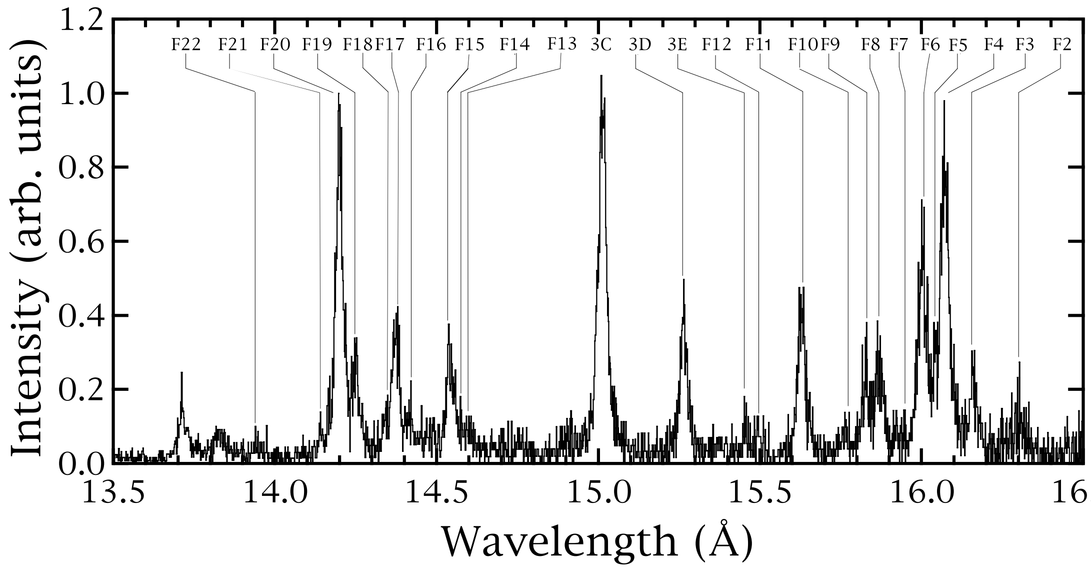


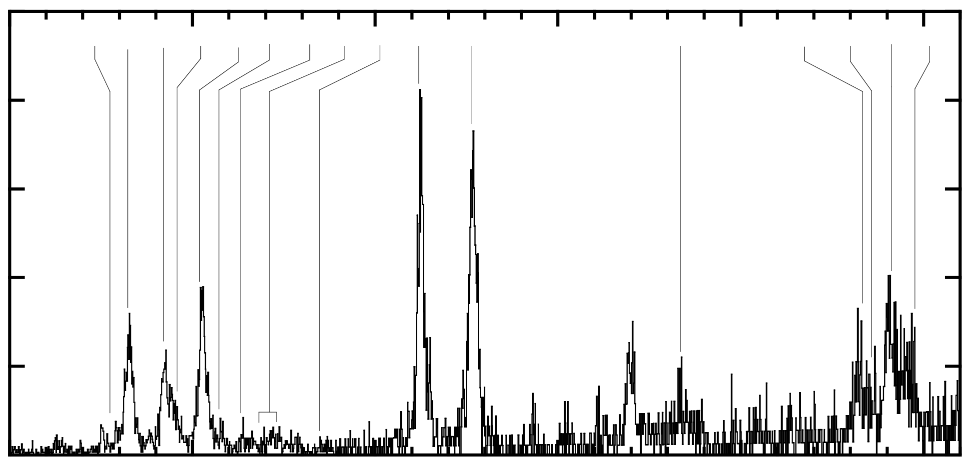

# LLNL EBIT Measurements of Fe Lines Below 10 Å

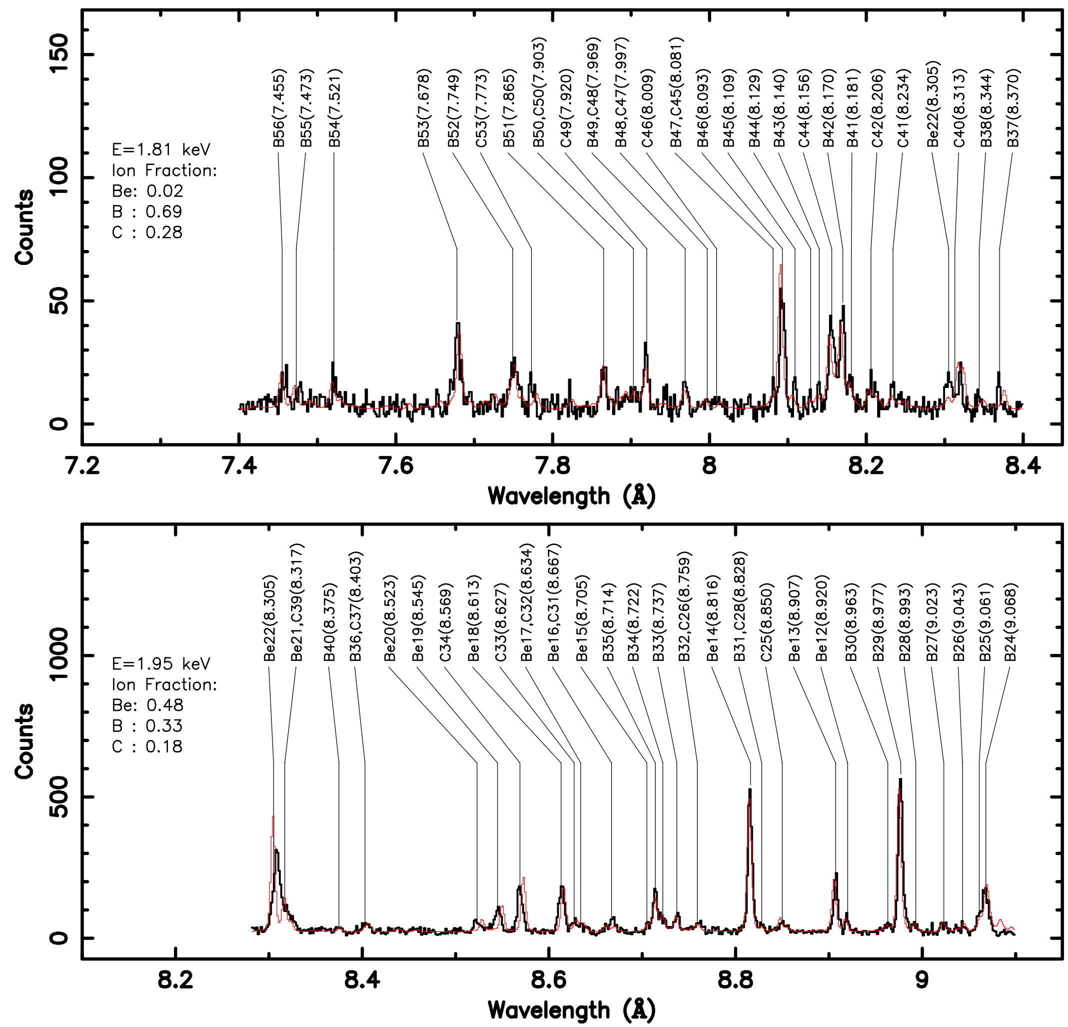


Chen et al. 2007

# LLNL EBIT Measurements of Ni Lines

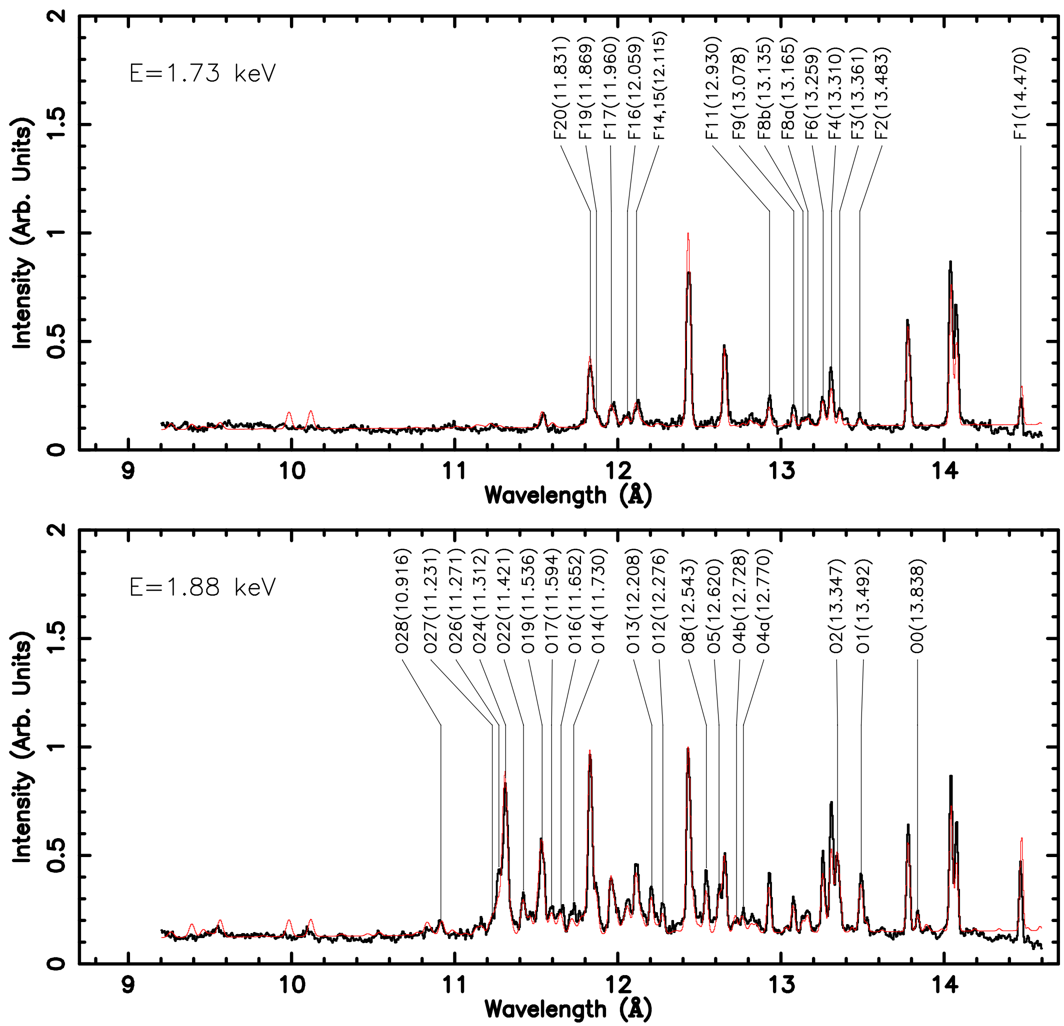


Gu et al. 2007

**LLNL EBIT Measurements of O VI and V Lines**

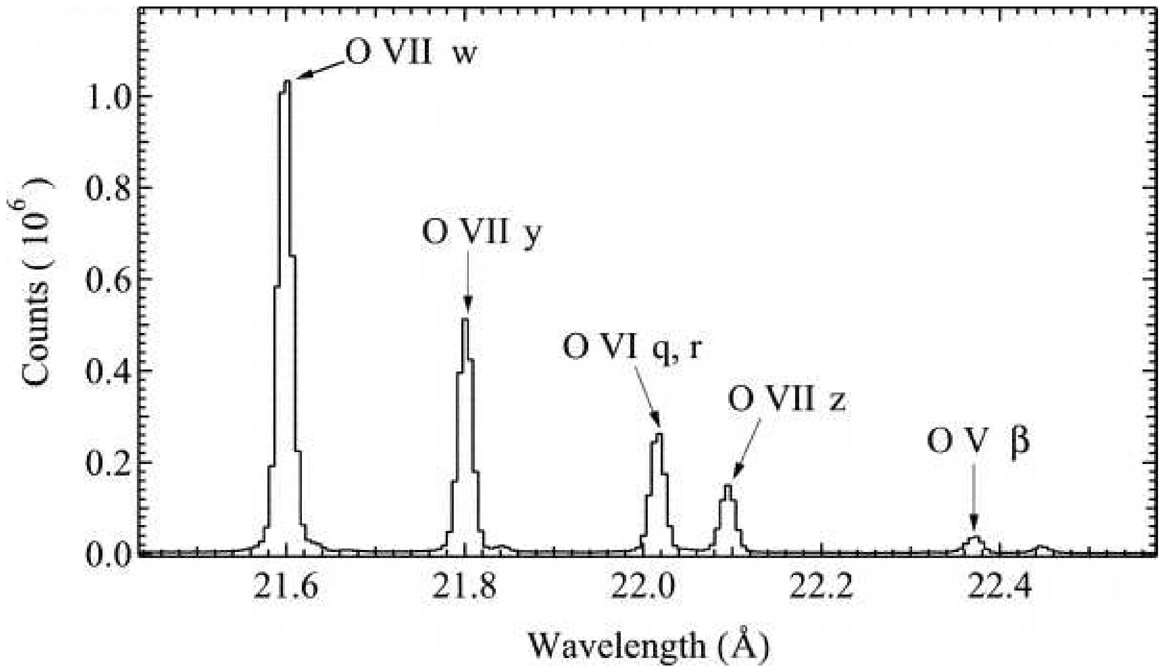


Schmidt et al., 2005

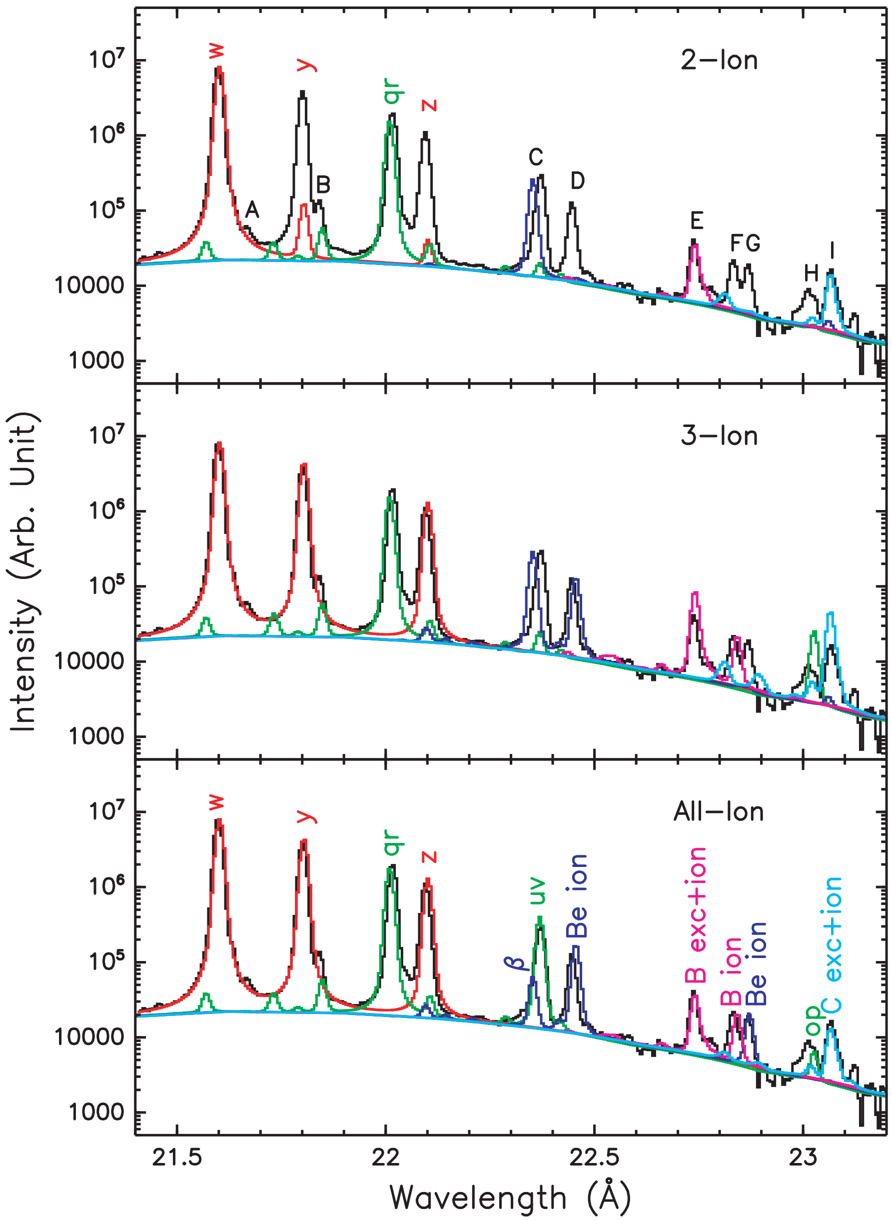

2−Ion
3−Ion
All−Ion
w
y
qr
z
A
B
C
D
E
FG
H
I
β
uv
Be ion
B exc+ion
B ion
Be ion
op
C exc+ion
Intensity (Arb. Unit)
Wavelength (Å)
21.5
22
22.5
23
10000
1000


Gu et al., 2005

**2nd order MBPT for Non-degenerate Single Level**

$$E_k =< \Phi_k|H|\Phi_k > +E^2,$$

where

$$E^2 = \sum_{n\neq k} \frac{\langle\Phi_k|H|\Phi_n\rangle\langle\Phi_n|H|\Phi_k\rangle}{E_k^0 - E_n^0}.$$

The general open shell ions, many levels are near degenerate. The interaction between these levels must be taken into account in all orders, leading to the multi-reference MBPT theory.

**Multi-reference MBPT Theory (Lindgren, JPB, 7, 2441)**

The exact energy and wavefunctions for the Hamiltonian $H_{DCB}$

$$H_{DCB}\Psi_k = E_k\Psi_k.$$

Split $H_{DCB} = H_0 + V$,

$$\begin{aligned} H_0 &= \sum_i [h_d(i) + U(r_i)] \\ V &= -\sum_i \left[\frac{Z}{r_i} + U(r_i)\right] + \sum_{i<j}\left(\frac{1}{r_{ij}} + B_{ij}\right). \end{aligned}$$

Define zeroth-order wavefunction and energy as the eigen functions $\Phi_k$ and eigen values $E_k^0$ of $H_0$, which are easily obtained by forming determinants from single-electron wavefunctions once $U(r)$ is given.

Devide the configuration space into $M$ and $N$. $M$ contains the levels of interest, and $N$ contains correlation configurations, usually, all single and double excitations from $M$.

Define a projection operator $P$,

$$\Psi_k^0 = P\Psi_k,$$

where $\Psi_k^0$ is generally a linear combination of the subset of $\Phi_k$ that belong to the model space $M$.

It is generally possible to define a wave operator, $\Omega$,

$$\Psi_k = \Omega\Psi_k^0.$$

Rewrite the Schrödinger equation

$$H_{eff}\Psi_k^0 = PH\Omega\Psi_k^0 = E_k\Psi_k^0.$$

This equation defines an effective Hamiltonian in the model space

$$H_{eff} = PH_0P + PV\Omega,$$

whose eigenvalues are the true eigenenergies of the full Hamiltonian. The effective Hamiltonian is generally non-hermitian, and the eigenfunctions, $\Psi_k^0$ are not necessarily orthogonal.

The starting point of the MBPT expansion

$$[\Omega, H_0] = V\Omega - \Omega V\Omega,$$

The potential $V\Omega$ up to irst order is

$$< \Phi_i|V\Omega|\Phi_j >=< \Phi_i|V|\Phi_j > + \sum_{r\in N} \frac{< \Phi_i|V|\Phi_r >< \Phi_r|V|\Phi_j >}{E_j^0 - E_r^0},$$

The first order effective Hamiltonian is then

$$< \Phi_i|H_{eff}^{(1)}|\Phi_j >= H_{DCB}^{ij} + \sum_{r\in N} \frac{V^{ir}V^{rj}}{E_j^0 - E_r^0},$$

Once the matrix $H_{eff}^{(1)}$ is determined, one may solve the generalized eigenvalue problem to obtain the 2nd-order MBPT energies.

## Numerical Evaluation of 2nd-order Expansion

$$
\begin{aligned}
V &= \sum Z^0(\alpha,\beta)V_{\alpha\beta} \\
&+ \sum (Z^k(\alpha,\gamma)\cdot Z^k(\beta,\delta)X^k(\alpha\beta,\gamma\delta) \\
\Delta H &= \sum_{r\in N} \frac{<\Phi_i|V|\Phi_r><\Phi_r|V|\Phi_j>}{E_j^0 - E_r^0} \\
\text{Num.} &= \sum_{config.} <\Phi_i|Z^0(\alpha,\beta)Z^0(\alpha',\beta')|\Phi_j> \\
&+ \sum_{config.} <\Phi_i|Z^0(\alpha,\beta)Z^k(\alpha',\gamma')\cdot Z^k(\beta',\delta')|\Phi_j> \\
&+ \sum_{config.} <\Phi_i|Z^k(\alpha,\gamma)\cdot Z^k(\beta,\delta)Z^0(\alpha',\beta')|\Phi_j> \\
&+ \sum_{config.} <\Phi_i|Z^k(\alpha,\gamma)\cdot Z^k(\beta,\delta)Z^k(\alpha',\gamma')\cdot Z^k(\beta',\delta')|\Phi_j>
\end{aligned}
$$

## Calculated energies of $1s^2 2l^q$ states of Ni and Fe

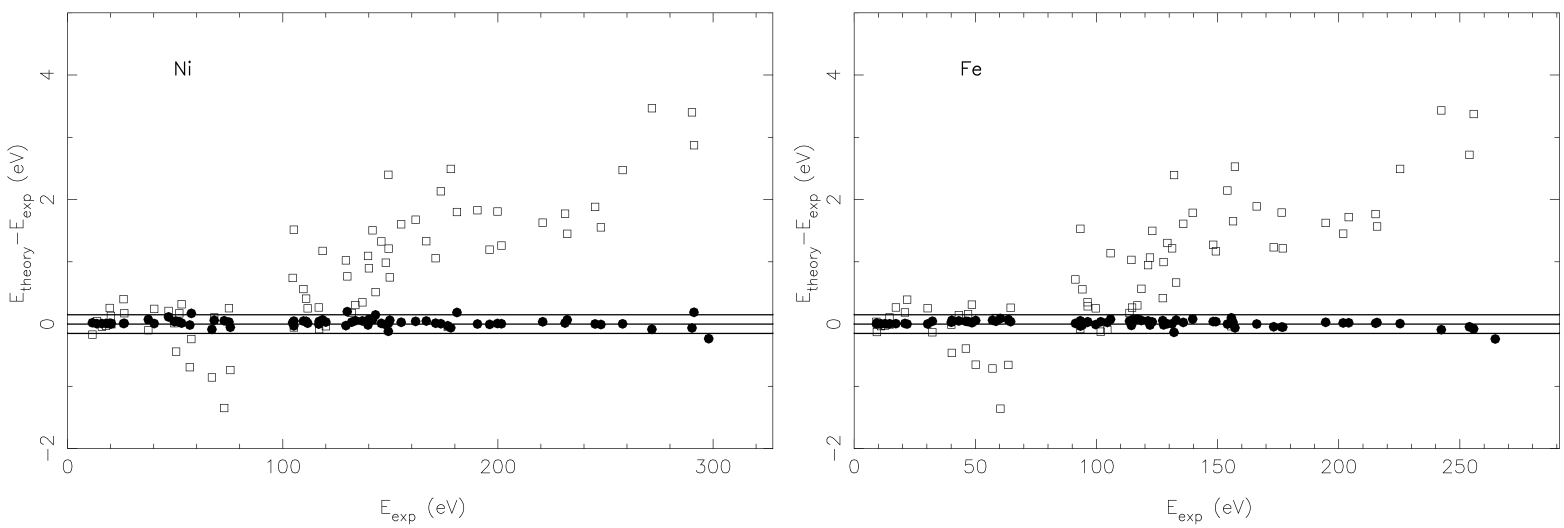

# Calculated wavelengths of 2–3 transitions of Fe L-shell ions

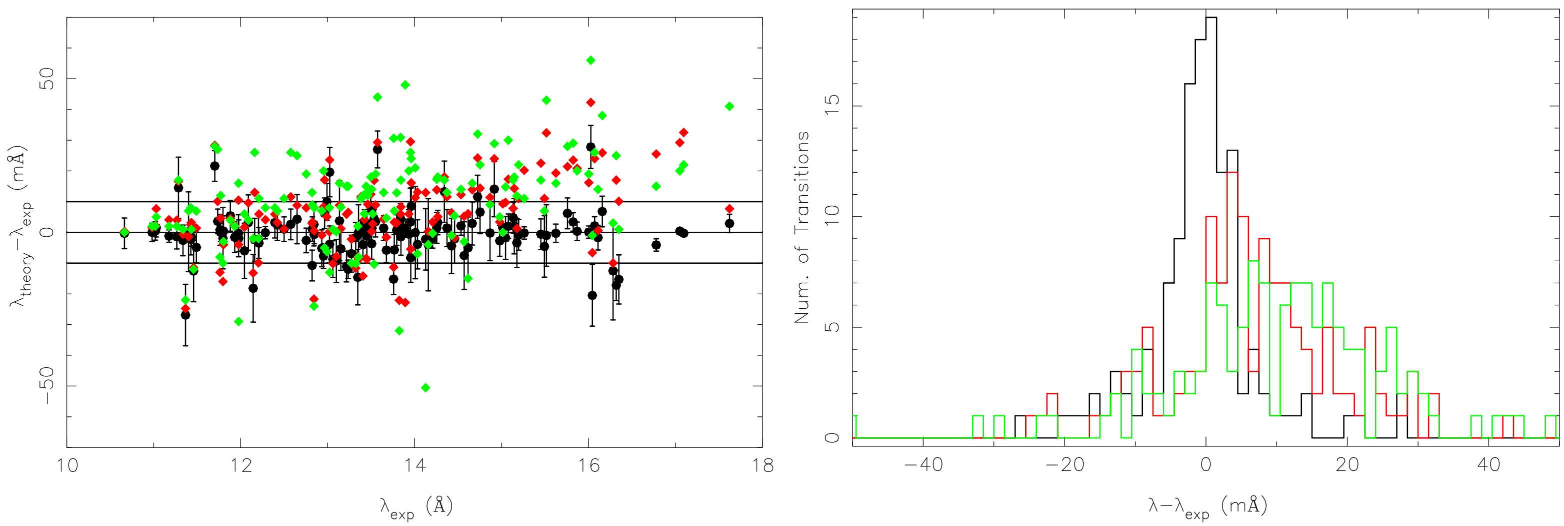

## MBPT Wavelengths and EBIT Measurements of Ni Lines

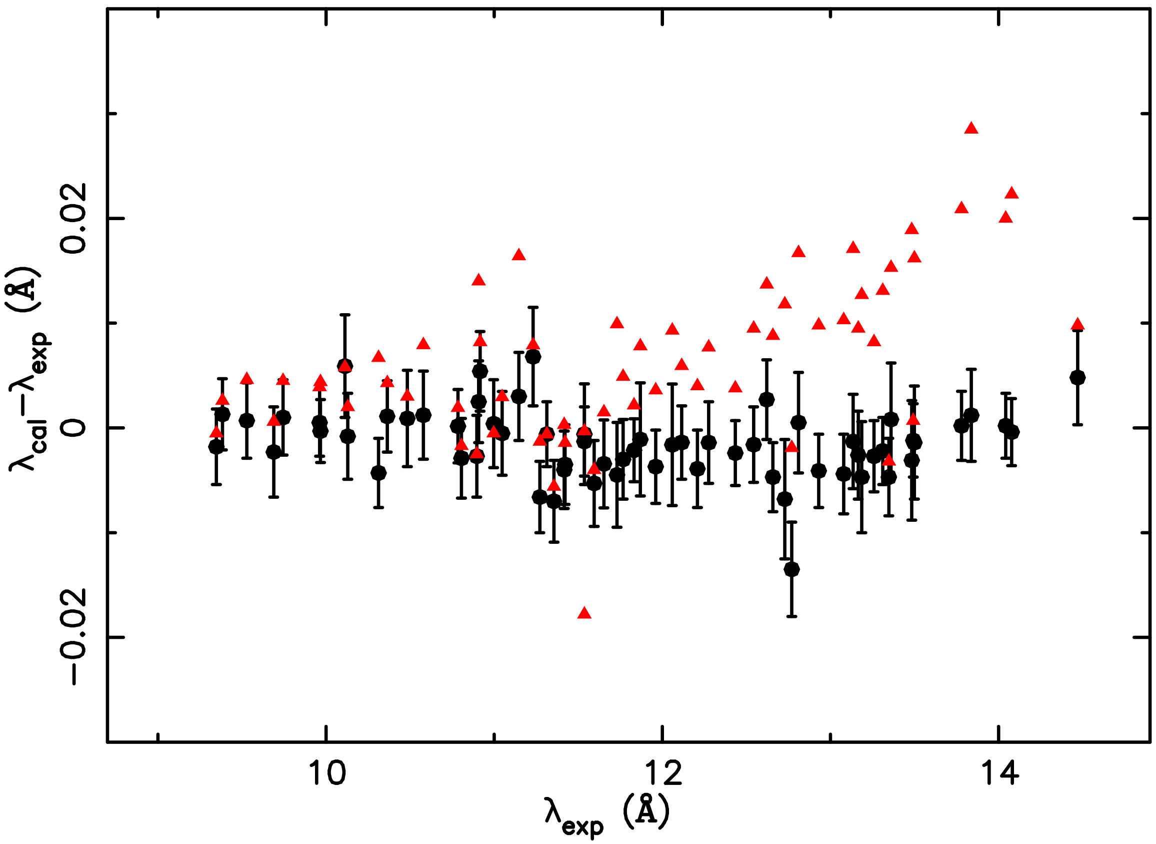


Gu et al., 2007

## MBPT Wavelengths and EBIT Measurements of Fe High-n Lines

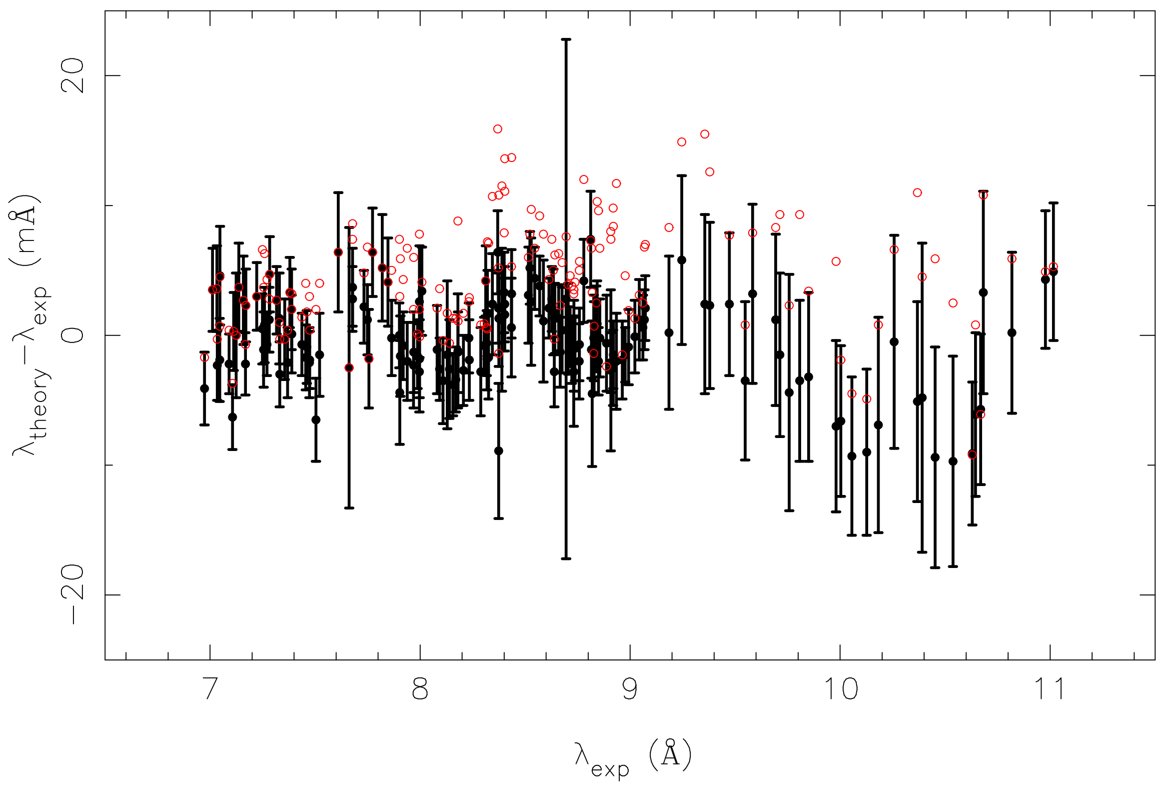


Gu 2007

## UTA transitions of iron M-shell ions

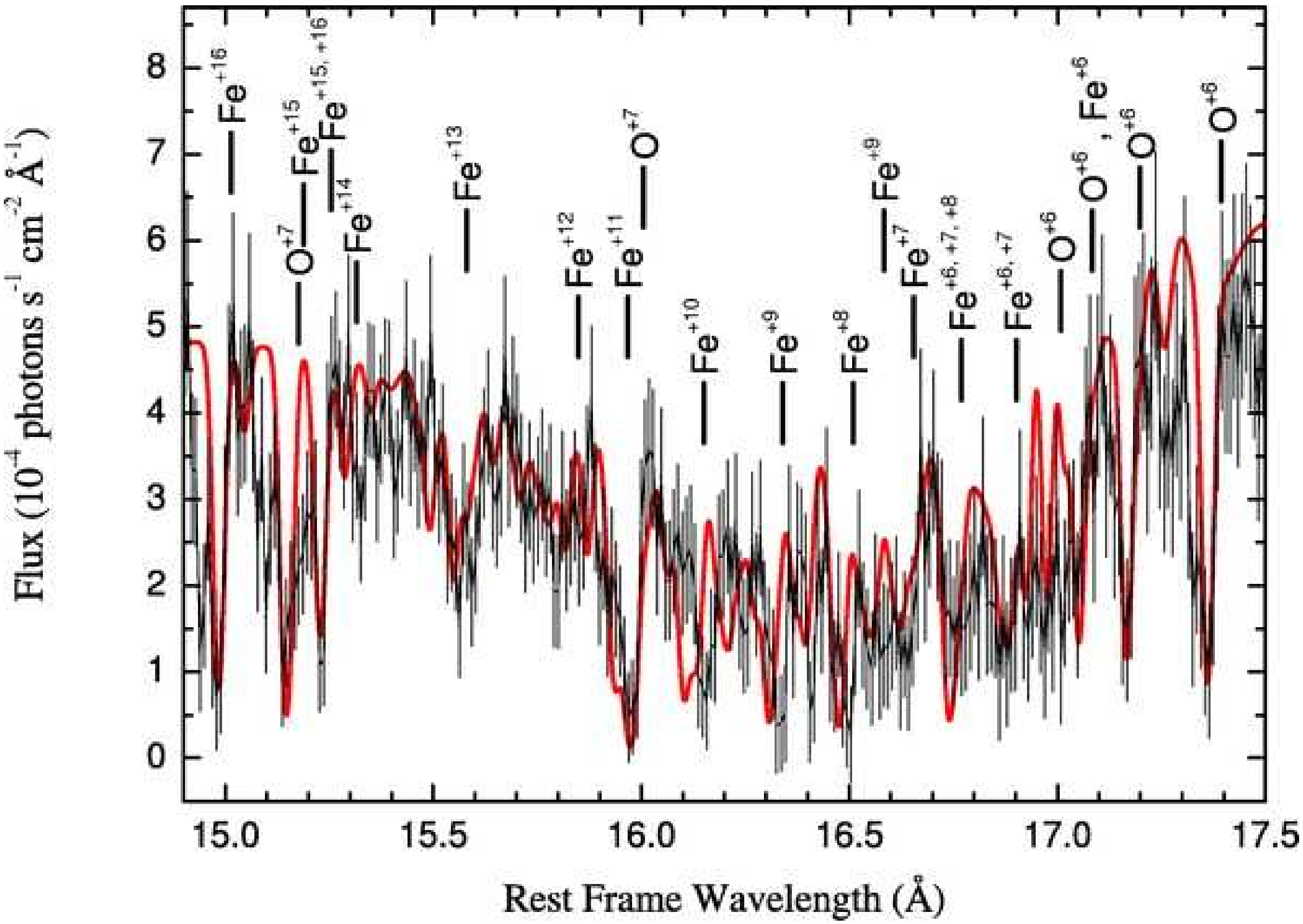


Holczer, Behar, & Kaspi, 2005

# Measuring the AGN Outflow Velocity with UTA

BEST-FIT VELOCITIES AND COLUMN DENSITIES FOR IONS DETECTED IN THE 14.9–17.5 Å REGION OF THE HETGS SPECTRUM OF NGC 3783

| Ion | $\lambda_{observed}$ (Å) | $\lambda_{rest}$[a] (Å) | $\lambda_{model}$[b] (Å) | Outflow Velocity[c] (km $s^{-1}$) | Ion Column Density ($10^{16}$ $cm^{-2}$) |
|---|---|---|---|---|---|
| $O^{+7}$ | 15.144 ± 0.003[d] | 15.176 | 15.146 | −633 ± 59 | 400 ± 60 |
| | 15.970 ± 0.005[e] | 16.006 | 15.973 | −675 ± 94 | ... |
| $O^{+6}$ | 17.351 ± 0.005 | 17.395 | 17.361 | −759 ± 81 | 110 ± 20 |
| | 17.161 ± 0.005 | 17.199 | 17.165 | −663 ± 89 | ... |
| | 17.048 ± 0.005 | 17.084 | 17.050 | −632 ± 88 | ... |
| $Fe^{+16}$ | 14.980 ± 0.003 | 15.013 | 14.985 | −659 ± 60 | 3.0 ± 0.5 |
| | 15.231 ± 0.002[f] | 15.261 | 15.234 | −590 ± 39 | ... |
| | | | Fe-M UTA | | |
| $Fe^{+15}$ | 15.231 ± 0.002[f] | 15.250 | 15.234 | −374 ± 39 | 0.6 ± 0.2 |
| $Fe^{+14}$ | 15.322 ± 0.006 | 15.316 | 15.317 | +118 ± 118 | 0.3 ± 0.1 |
| $Fe^{+13}$ | 15.569 ± 0.008[g] | 15.580 | 15.580 | +212 ± 154 | 1.4 ± 0.4 |
| $Fe^{+12}$ | 15.844 ± 0.014[g] | 15.848 | 15.848 | −76 ± 265 | 1.0 ± 0.3 |
| $Fe^{+11}$ | 15.970 ± 0.005[e] | 15.967 | 15.973 | +56 ± 94 | 3.0 ± 2.0 |
| $Fe^{+10}$ | 16.154 ± 0.005 | 16.150 | 16.150 | +74 ± 93 | 4.0 ± 0.7 |
| $Fe^{+9}$ | 16.329 ± 0.005 | 16.339 | 16.340 | −184 ± 92 | 5.5 ± 0.7 |
| $Fe^{+8}$ | 16.496 ± 0.004 | 16.510 | 16.509 | −252 ± 73 | 4.0 ± 0.5 |
| $Fe^{+7}$[h] | ... | 16.655 | ... | ... | 3.0 ± 1.0 |
| $Fe^{+6}$[h] | ... | 17.095 | ... | ... | 2.0 ± 0.7 |
| $Fe^{+5}$[h] | ... | 17.218 | ... | ... | 1.5 ± 0.6 |
| $Fe^{+4}$[h] | ... | 17.291 | ... | ... | 1.0 ± 0.6 |
| $Fe^{+3}$[h] | ... | 17.405 | ... | ... | $\leq$0.8 |

Holczer, Behar, & Kaspi, 2005

## Comparison of MBPT and HULLAC Wavelengths for Fe UTA

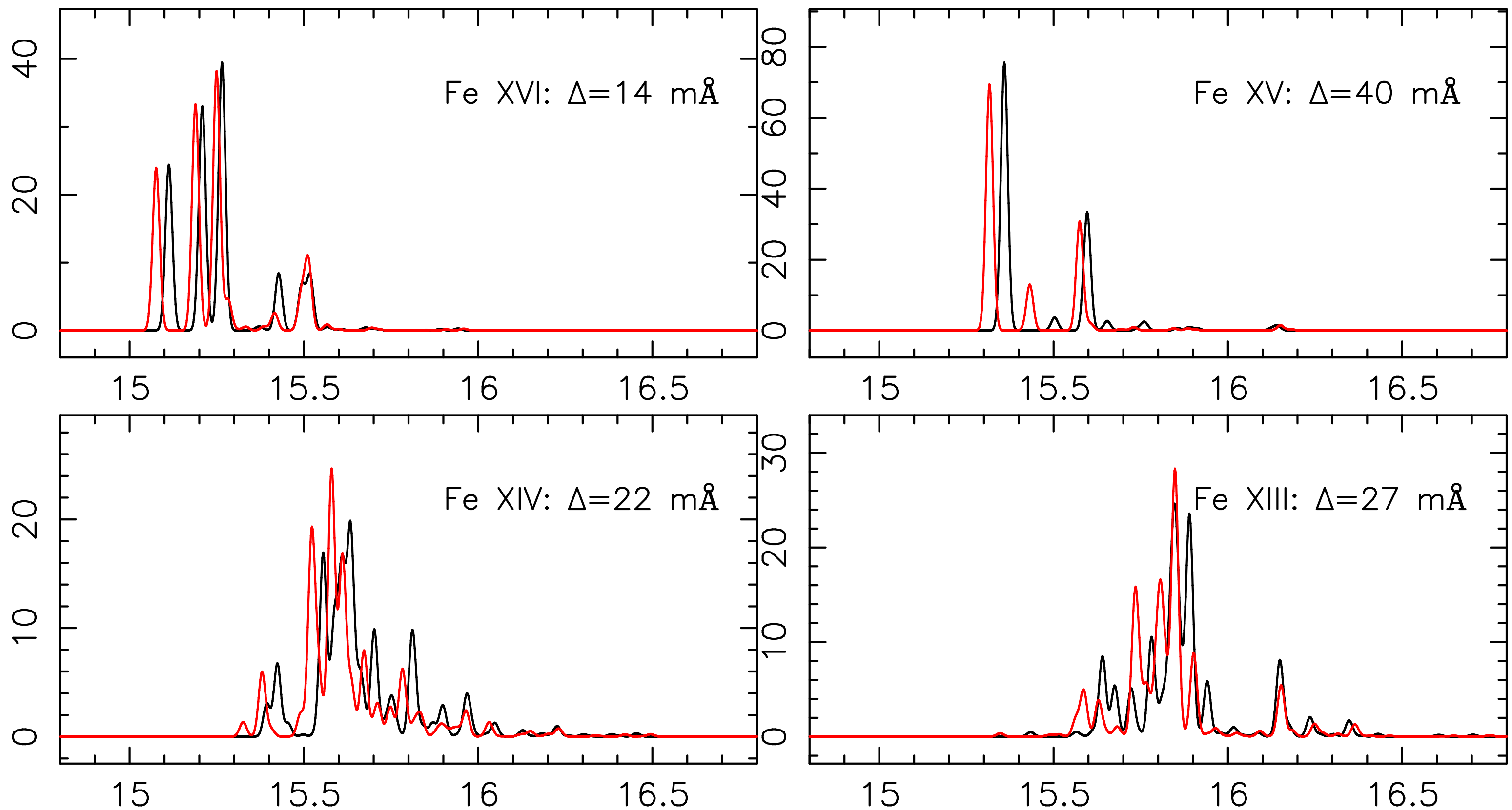

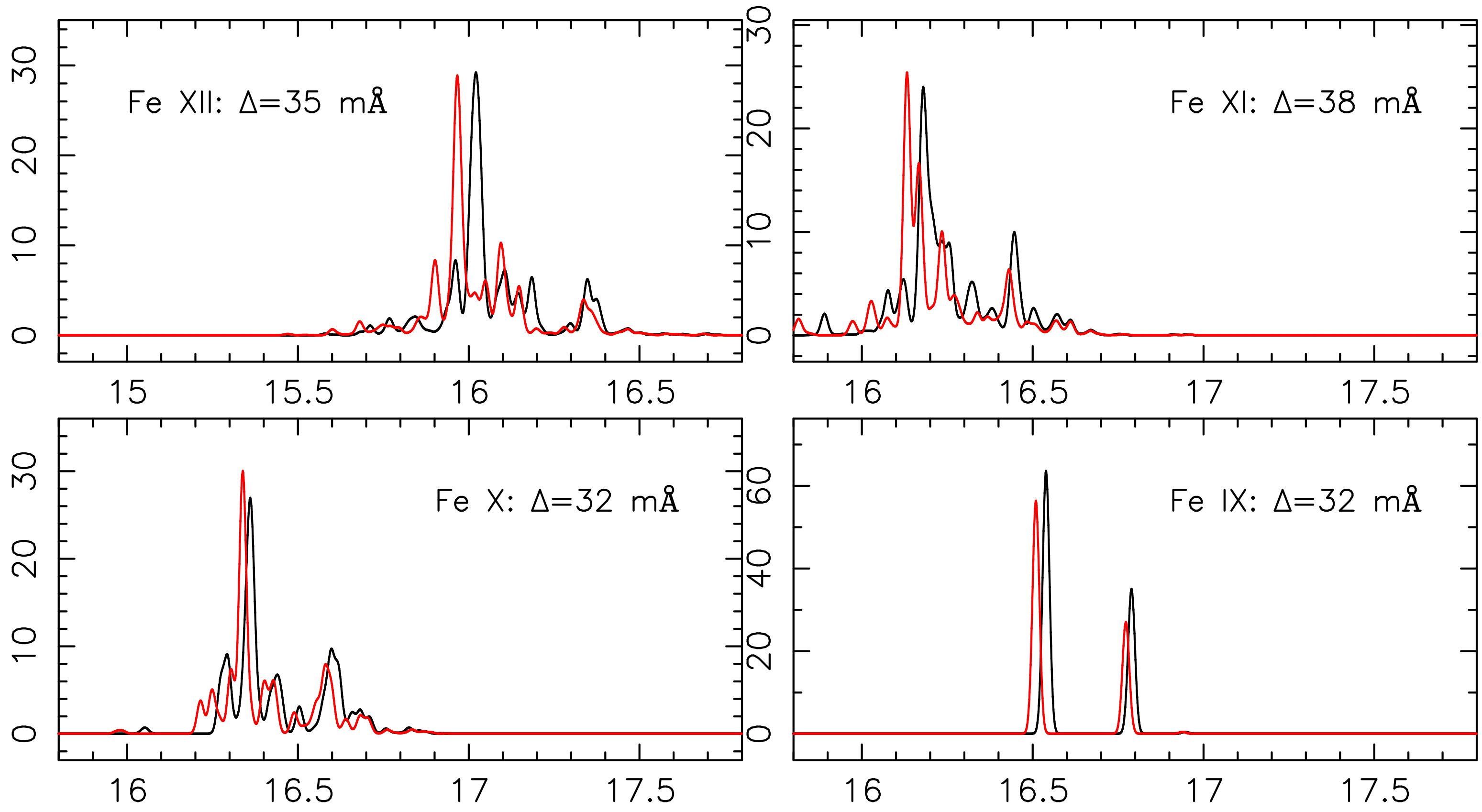
Fe XII: Δ=35 mÅ
Fe XI: Δ=38 mÅ
Fe X: Δ=32 mÅ
Fe IX: Δ=32 mÅ

## Comparison of MBPT data with NGC 3783

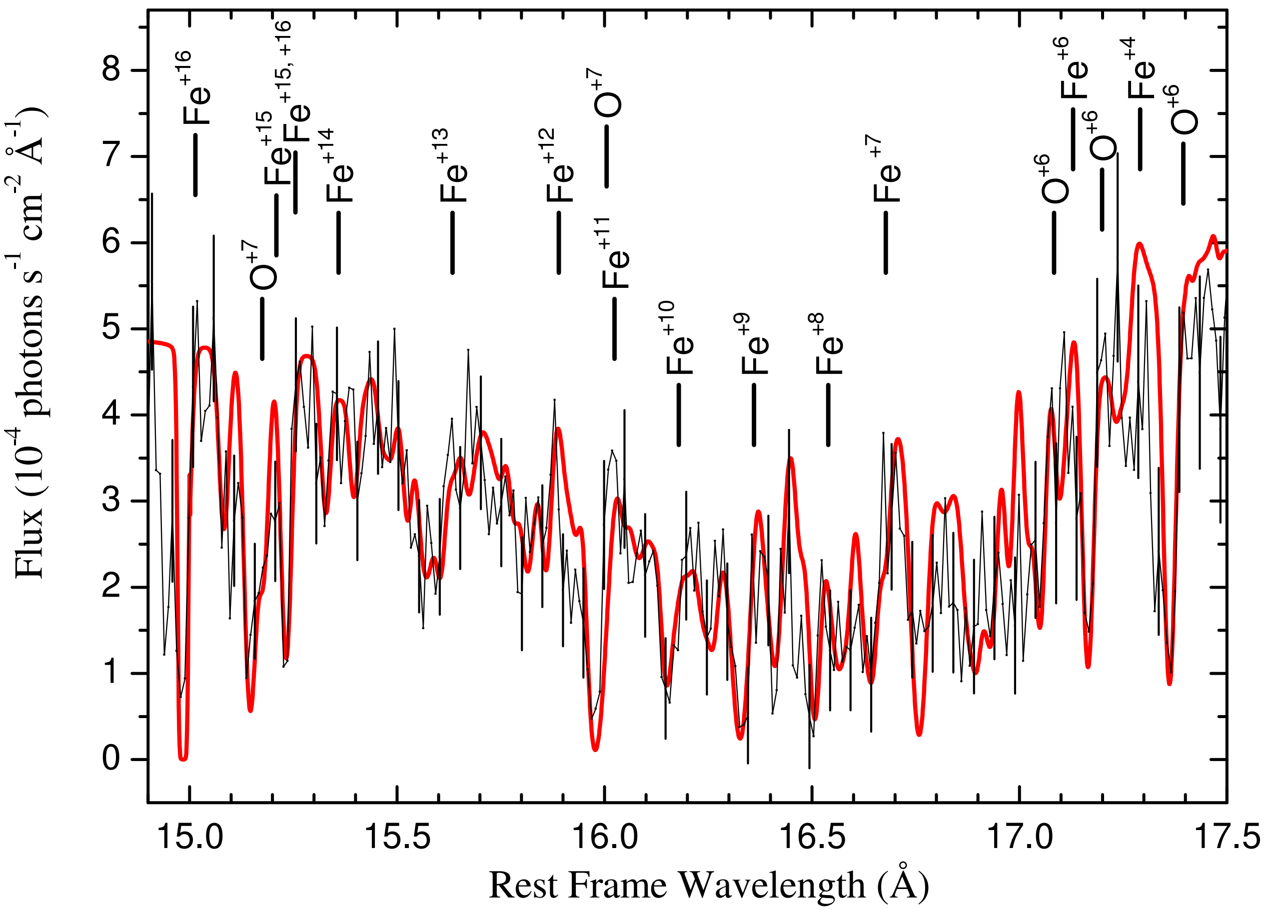


Gu et al., 2006, Consistent velocity measurements.

## Summary

- LLNL EBIT measurements of X-ray wavelengths have made significant contributions to the field.
- Many-body perturbation theory has been implemented in the Flexible Atomic Code.
- MBPT wavelengths reaches wavelengths accuracy matching the spectral resolutions of the X-ray observatories.
- Future measurements of K-shell transitions of Ne, Mg, Si, and S, and L-shell tranistions of Fe UTA.
- Future calculations of K-shell transitions of O, Ne, Mg, Si, and S.